Acta Geodyn. Geomater., Vol. 17, No. 2 (198), 207–215, 2020
DOI: 10.13168/AGG.2020.0015
journal homepage: https://www.irsm.cas.cz/acta

ORIGINAL PAPER

PERIOD AND *Q*-FACTOR OF FREE CORE NUTATION, BASED ON DIFFERENT GEOPHYSICAL EXCITATIONS AND VLBI SOLUTIONS

Jan VONDRÁK * and Cyril RON

Department of Galaxies and Planetary Systems, Astronomical Institute, Czech Academy of Sciences, Boční II, 141 00 Prague 4, Czech Republic

Corresponding author's e-mail: vondrak@ig.cas.cz

ARTICLE INFO

Article history:
Received 18 December 2019
Accepted 26 March 2020
Available online 8 April 2020

Keywords:
Rotation of the Earth
Geophysical excitations
Geomagnetic jerks
VLBI
Celestial pole offsets
Free core nutation

ABSTRACT

Three variants of geophysical excitations and seven different VLBI solutions of celestial pole offsets (CPO) are used to determine period and *Q*-factor of Free Core Nutation (FCN). Brzeziński's broad-band Liouville equations (Brzeziński, 1994) are numerically integrated to derive geophysical effects in nutation in time domain. Possible effect of geomagnetic jerks (GMJ) is also considered. Best-fitting values of FCN parameters are estimated by least-squares fit to observed CPO, corrected for the differences between the FCN parameters used in IAU 2000 model of nutation and newly estimated ones; MHB transfer function is used to compute these corrections. It is demonstrated that different VLBI solutions lead to FCN parameters that agree on the level of their formal uncertainties, but different models of geophysical excitations change the results more significantly. Using GMJ excitations always brings improvement of the fit between integrated and observed CPO. The obtained results show that the best fit is achieved when only GMJ excitations are used. Our conclusion is that GMJ are very probably more important for exciting FCN than the atmosphere and oceans. Empirical Sun-synchronous correction, introduced in the present IAU 2000 nutation model, cannot be explained by diurnal atmospheric tidal effects.

1. INTRODUCTION

It is well known that the main part of nutation is caused by external torques, dominantly exerted by the Moon, Sun, and to a smaller extent also by planets. Model of nutation IAU2000, presently adopted as standard by the IAU, is based namely on these forces for rigid Earth (Souchay et al., 1999), and further modified by Mathews et al. (2002) for the effect of the Earth's non-rigidity. Excitations by geophysical fluids (atmosphere, oceans) are neglected since they play much smaller role and cannot be predicted, but they are now detectable by VLBI. The same holds for the FCN. Rapid changes of amplitude & phase of this free term occur near the epochs of GMJ (rapid changes of the second time derivatives of intensity of geomagnetic field), as demonstrated by Malkin (2013).

In the past, many authors used different observation techniques and methods of analysis to derive FCN parameters (period *T* and *Q*-factor), both with and without geophysical excitations included. In principle, there are two different types of observation, used for this purpose:

a) Tidal gravity data, using superconducting gravimeters. Here we can name at least some results – Defraigne et al. (1994), Florsch and Hinderer (2000), Hinderer et al. (2000), or Cui et al. (2018).

b) VLBI observations that provide the differences between real motion of the Earth's spin axis in space and the adopted model of nutation – CPO. Interesting results were obtained, e.g., by Mathews et al. (2002), used in the IAU model of nutation, Vondrák et al. (2005), Rosat and Lambert (2009), who used also gravimetric observations, Gubanov (2010), Koot and de Viron (2011), Huang et al. (2011), Krásná et al. (2013), Chao and Hsieh (2015), Zhou et al. (2016) or Vondrák and Ron (2017, 2019).

We have recently developed a new method of determining FCN parameters from VLBI observations, considering geophysical excitations (Vondrák and Ron, 2017). The motivation of the study presented here is to show how much geophysical excitations from different models and different VLBI solutions of CPO are reflected in derived FCN parameters. To this end, we use here namely this method, and compare the results with other determinations.

Cite this article as Vondrák J, Ron C: Period and *Q*-factor of free core nutation, based on different geophysical excitations and VLBI solutions. Acta Geodyn. Geomater., 17, No. 2 (198), 207–215, 2020. DOI: 10.13168/AGG.2020.0015

2. DESCRIPTION OF THE METHOD

Only the main points of the method are outlined below, for more details we refer the reader to our previous work (Vondrák and Ron, 2017).

We use broad band Liouville equations (Brzeziński, 1994) in celestial reference frame

$$\ddot{P} - \mathrm{i}(\sigma'_c + \sigma'_f)\dot{P} - \sigma'_c\sigma'_f P =$$
$$= -\sigma_c\left\{\sigma'_f\left(\chi'_p + \chi'_w\right) + \sigma'_c\left(a_p\chi'_p + a_w\chi'_w\right) + \mathrm{i}\left[(1+a_p)\dot{\chi}'_p + (1+a_w)\dot{\chi}'_w\right]\right\}, \quad (1)$$

to integrate numerically the influence of geophysical excitations. This differential equation is given in complex form, $P = \mathrm{d}X + \mathrm{i}\mathrm{d}Y$ denotes the motion of celestial pole due to excitations, σ_c, σ'_c are complex Chandler frequencies in terrestrial and celestial frame, respectively, σ'_f is the FCN frequency in celestial frame. All frequencies are expressed in radians per day. χ'_p, χ'_w are excitations (in celestial frame) due to pressure (matter) and wind (motion), respectively. Dimensionless numerical constants that we use here $a_p = 9.200 \times 10^{-2}$, $a_w = 2.628 \times 10^{-4}$, expressing different reaction on pressure and wind terms, slightly differ from those originally recommended by Brzeziński (1994). They follow from some more recent parameters found by Koot and de Viron (2011), see also Schindelegger et al. (2013). The relation between complex frequency σ'_f and FCN parameters T, Q is given as

$$\sigma'_f = -\frac{2\pi}{T}\left[1 - \frac{\mathrm{i}(1+1.00273T)}{2Q}\right]. \quad (2)$$

To integrate equation (1), we use standard atmospheric and oceanic excitations from different sources, the additional effect of geomagnetic jerks is modeled by impulse-like excitation functions whose amplitudes are determined to yield the best agreement with observations (see the next section). We then find FCN parameters that yield the best fit between integrated and observed CPO values, using standard least-squares estimation.

According to Mathews et al. (2002), the amplitudes and phases of individual nutation terms depend on their frequencies and, among other factors, also on the complex FCN frequency, and therefore on the FCN parameters T, Q that we are looking for. The relation is given by so called MHB transfer function

$$T_{MHB}(\sigma) = \frac{e_r - \sigma}{e_r + 1} N_0\left[1 + (1+\sigma)\left(Q_0 + \sum_{j=1}^{4}\frac{Q_j}{\sigma - s_j}\right)\right], \quad (3)$$

in which σ denotes the frequency of a nutation term, e_r dynamical ellipticity of the rigid Earth, N_0, Q_j are complex numerical constants, and s_j are complex resonance frequencies. All frequencies are expressed in cycles per sidereal day. Out of these, namely s_2 corresponds to FCN, and is related to σ'_f by a simple relation $s_2 = \sigma'_f/\Omega - 1$, in which $\Omega = 6.30038$ is the mean speed of Earth's rotation in radians per day. We use expressions (2) and (3) to re-calculate nutation from standard values T=430.21d, Q=20000 to the newly estimated one, and correct the corresponding CPO. They are then used, in successive approximations, to find the FCN parameters leading to the best fit (in least-squares sense) with the integrated values. In parallel to these, initial position of the pole must also be found. In case when GMJ effect is included, eight more complex values of excitation amplitudes a (see Eq. (4) in the next section) are to be estimated.

3. THE DATA

We use here the following data, all available in interval 1986.0-2018.5 at IERS website:

A. Celestial pole offsets data in 1-day steps:

- Combined solutions:
  - IERS C04 combined solution eopc04_IAU2000.dat (C04);
  - IVS combined solution ivs18q2X.eops (IVS);
- Individual solutions by IVS analytical centers:
  - Bundesamt für Kartografie und Geodäsie bkg00014.eoxy (BKG);
  - Goddard Space Flight Center gsf2016a.eoxy (GSF);
  - Institute for Applied Astronomy iaa2017a.eops (IAA);
  - Observatoire de Paris opa2019a.eops (OPA);
  - U.S. Naval Observatory usn2019c.eoxy (USN).

All data are filtered to contain periods between 10 and 6000 days, using the filter by Vondrák (1977), and further corrected by using MHB transfer function, as described in preceding section. In accordance with our last papers (Vondrák and Ron, 2017, 2019) we keep MHB empirical prograde annual Sun-synchronous correction

(SSC) in nutation model. Unlike in our older studies, in which we were removing this term, its application proved to yield better results.

B. Atmospheric and oceanic excitations:

- No atmospheric and oceanic excitations;
- NCEP/NCAR atmosphere with IB correction (which represents a simple oceanic model), in 6-hour steps (Zhou et al., 2006). Oceanic ECCO excitation model (Gross, 2009) cannot be used in this case, because it lacks near diurnal signal in terrestrial frame (which becomes long-periodic in celestial frame). Thus it is important for exciting only polar motion, not nutation; see also our comment in (Vondrák and Ron, 2015).
- ESM GFZ atmosphere + ocean, in 3-hour steps (Dobslaw and Dill, 2018, Jungclaus et al., 2013).
- ESM GFZ corrected – the same as above, with atmospheric diurnal tidal components (S1, P1, K1), originally removed from the excitations, restored. To this end, we use the information given in Tables 7.1 and 7.2 of Product Description Document (Dobslaw and Dill, 2019). Oceanic excitations could not be restored in a similar way because the necessary information is missing. These diurnal components, after transformation into the celestial reference frame, contribute to prograde annual nutation, so we use corrected excitations also in combination with CPO without SSC.

All data, originally given in terrestrial frame, were re-calculated into celestial frame, centered and smoothed to contain only periods longer than 10 days.

C. Geomagnetic jerks. Eight epochs of GMJ within the time interval studied, are used:

- 1991.0 (Malkin, 2013);
- 1994.0 (Malkin, 2013);
- 1999.0 (Malkin, 2013);
- 2003.5 (Olsen and Mandea, 2008);
- 2004.7 (Mandea et al., 2010)
- 2007.5 (Malkin, 2013);
- 2011.0 (Chulliat and Maus, 2014);
- 2014.0 (Brown et al. 2016).

A possible physical mechanism between FCN and GMJ can probably be found in changes of core-mantle electromagnetic coupling (Cui et al., 2018). However, the conclusions about their exact relationship cannot be made so far, as concluded, e.g., by Cui et al. (2020). Therefore, we simply model the excitations by the expression

$$\chi'_{GMJ} = \frac{a}{2}\left[1 + \cos\frac{2\pi(t-t_0)}{200}\right]. \quad (4)$$

The complex amplitudes a of an impulse-like, bell-shaped excitations, centered around the fixed GMJ epochs and lasting 200 days, are estimated from the fit to observations. As we demonstrated earlier (Vondrák and Ron, 2015), this form of schematic excitation is capable of changing both phase and amplitude of FCN, without affecting the mean position of the pole. And this is exactly what we see from the observations.

As the Brzeziński's broad-band Liouville equations (1) address mass transport at the Earth's surface, they are probably not fully adequate to model hypothetic GMJ effect by core-mantle coupling. In spite of this, we use these equations even in this case since we believe they can still yield reasonable results for integrated pole position. The values of amplitudes a of Eqs. (4) have however unclear physical relation to core/mantle torque.

4. RESULTS

Using different combinations of seven CPO series with three sources of atmospheric/oceanic excitations leads to 46 different solutions, provided they are made both with and without GMJ effects; all results are shown in Table 1. The last two rows, with corrected GFZ excitations (see preceding section) show the results with CPO from C04 solutions only.

All results of Table 1, with the exception of the last two rows (see comment below) are graphically depicted in Figures 1 through 3. A common feature of all three figures is that solutions with different CPO series agree within their formal uncertainties, if the same excitation model is used. The best rms fit is always achieved with C04 series, and it is improved substantially in all cases (see columns rms of Table 1) when GMJ effect is added.

If no atmospheric and oceanic excitation is used, the inclusion of GMJ effect does not practically change the value of Q-factor, and period T is shortened by less than one day, as demonstrated in Figure 1.

Figure 2 offers a different pattern than Figure 1; all rms fits are slightly worse, Q-factor is systematically larger, inclusion of GMJ diminishes it by about 1000, while period does not change very much.

Results of Figure 3 yield the highest values of rms fits, but these are significantly reduced when GMJ effect is accounted for. Both parameters, period T and Q-factor, are much different from preceding two cases; the former is shorter by about 0.3d (with GMJ excitation even more), the latter is larger by almost 3000 when GMJ excitation is added.

Solutions with corrected GFZ excitations are not displayed separately since they would not be graphically distinguishable from the values of Figure 3.

Comparison of integrated with observed CPO is shown in Figures 4 – 7; only the solutions with IERS C04 are depicted for the four variants of atmospheric/oceanic excitations, respectively. Solutions without (top) and with (bottom) GMJ effect are displayed, GMJ epochs are marked with arrows.

Table 1 Solutions of FCN parameters *T, Q* for different combinations of CPO and atmospheric/oceanic excitations.

A+O excitations	analysis center	with GMJ			without GMJ		
		T	*Q*	rms [mas]	*T*	*Q*	rms [mas]
no A+O excitation	BKG	430.33±0.04	19900±180	0.227	430.40±0.05	19900±220	0.280
	C04	430.23±0.03	19600±170	0.166	430.36±0.04	19700±190	0.232
	GSF	430.29±0.04	19800±180	0.225	430.39±0.05	19900±220	0.280
	IAA	430.20±0.04	19800±170	0.220	430.30±0.05	20000±220	0.273
	IVS	430.30±0.04	19900±180	0.219	430.38±0.05	19900±220	0.270
	OPA	430.24±0.04	19600±180	0.223	430.33±0.05	19700±220	0.272
	USN	430.25±0.04	19700±160	0.204	430.37±0.05	19800±210	0.259
NCEP IB	BKG	430.26±0.05	21700±230	0.241	430.27±0.06	22700±310	0.291
	C04	430.17±0.04	21400±180	0.188	430.22±0.05	22300±250	0.246
	GSF	430.23±0.05	21600±230	0.237	430.25±0.07	22500±370	0.351
	IAA	430.14±0.04	21800±220	0.234	430.15±0.07	22900±370	0.341
	IVS	430.25±0.05	21700±230	0.237	430.25±0.05	22700±300	0.282
	OPA	430.22±0.05	21500±230	0.243	430.14±0.06	22400±300	0.287
	USN	430.22±0.04	21600±210	0.224	430.24±0.05	22500±290	0.274
GFZ	BKG	429.64±0.05	22100±240	0.251	429.91±0.08	19400±340	0.445
	C04	429.61±0.04	21800±190	0.197	429.87±0.08	19100±300	0.414
	GSF	429.61±0.05	22100±240	0.247	429.91±0.08	19400±340	0.443
	IAA	429.50±0.05	22300±240	0.246	429.81±0.08	19600±340	0.443
	IVS	429.62±0.05	22100±230	0.242	429.89±0.08	19400±330	0.437
	OPA	429.55±0.05	21900±240	0.247	429.82±0.08	19200±320	0.437
	USN	429.58±0.04	22000±220	0.230	429.89±0.08	19300±320	0.431
GFZ_corr	C04	429.65±0.04	21800±200	0.215	429.91±0.08	19100±310	0.421
	C04_noSSC	429.63±0.04	21800±200	0.206	429.92±0.08	19100±310	0.419

Figure 4 displays the solutions with no atmospheric/oceanic excitations. The first glance at the upper plot (with no excitations at all) reveals slowly damped motion, corresponding to FCN with parameters *T, Q*, shown at the heading, and surprisingly small amplitude. Integration evidently differs from the observations, but the rms fit is still relatively small. A closer look at the results however discloses that the observed variations of CPO have substantially different period (around 450 days) from the best-fitting one, and a variable amplitude. Should this period be used, the corrected CPO values would be much more different and yield higher rms value. Substantial difference between resonant and directly observed period of FCN is already known (see, e.g., Vondrák et al., 2005). The discrepancies however almost disappear when GMJ excitations are considered (compare with lower plot); the estimated values of amplitudes a of GMJ effect are in the range between 0.10 and 1.65 mas. Thus the difference in period estimated from the resonance and direct method can be very probably ascribed to the influence of GMJ.

Solutions with IERS IB excitations are shown in Figure 5. The excitations of dominant pressure term χ'_p used here have peak amplitudes up to 3 mas. The agreement between integrated and observed values of CPO is slightly worse than in the preceding case and again, it is much improved when GMJ effect is considered. The estimated amplitudes a of additional excitations by GMJ are slightly higher than in the preceding case, between 0.28 and 1.66 mas.

Figure 6 displays the results of integration with ESM GFZ excitations by the atmosphere and oceans. The excitations (pressure term) are more than two times larger than the ones of NCEP IB model (peak amplitudes reach up to 7.40 mas). Consequently, the fit to observed CPO values is worse than in both preceding cases. On the other hand, the improvement achieved by including GMJ effect is very large; rms fit diminishes to less than one half (compare rms fits of upper and lower plot). The estimated amplitudes of GMJ excitation are much higher than in the preceding case, they are between 0.46 and 3.47 mas, so it seems that they partly compensate the influence of atmosphere and oceans.

Figure 7 shows the results of integration with corrected ESM GFZ excitations (diurnal atmospheric tidal components S1, P1, K1 restored), in combination with C04 CPO without SSC term. Evidently, the results are almost identical with preceding case, differences from Figure 6 are quite negligible. Diurnal atmospheric tides, restored in ESM GFZ excitations, do not contribute to final results significantly, being too far from FCN resonance.

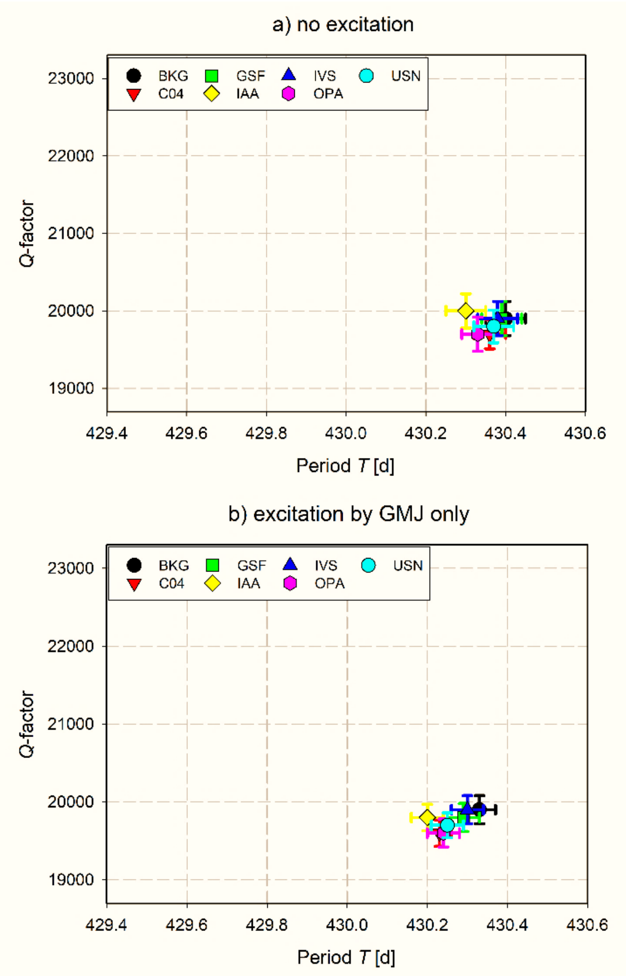

Fig. 1 FCN parameters from the solutions without atmospheric and oceanic excitations.

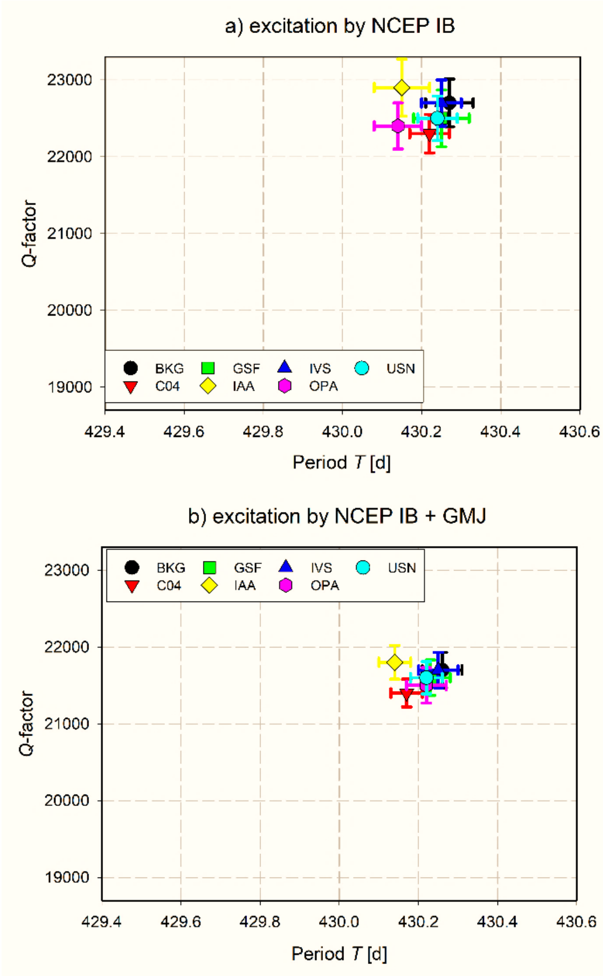

Fig. 2 FCN parameters from the solutions with NCEP IB excitations.

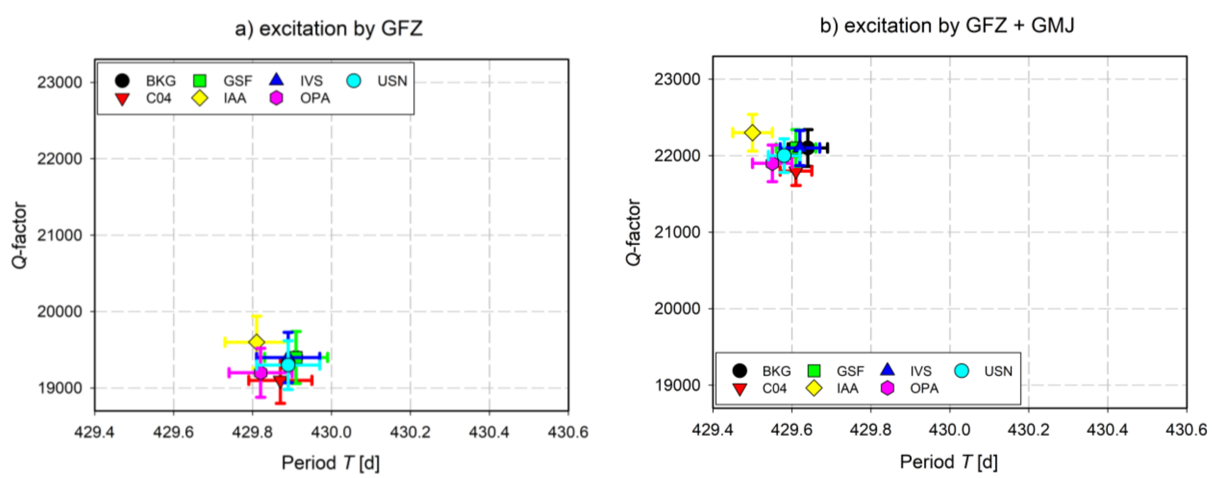

Fig. 3 FCN parameters from the solutions with GFZ excitations.

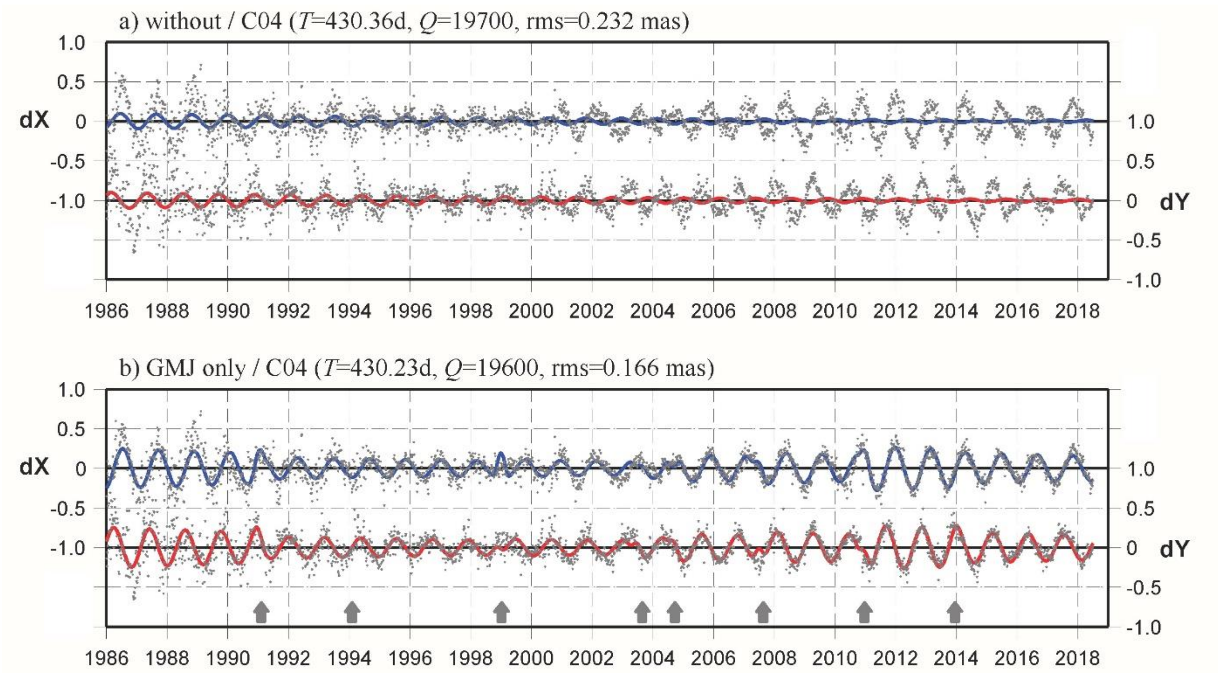

Fig. 4 Integrated (full lines) and observed (dots) CPO. No atmospheric and oceanic excitations are used.

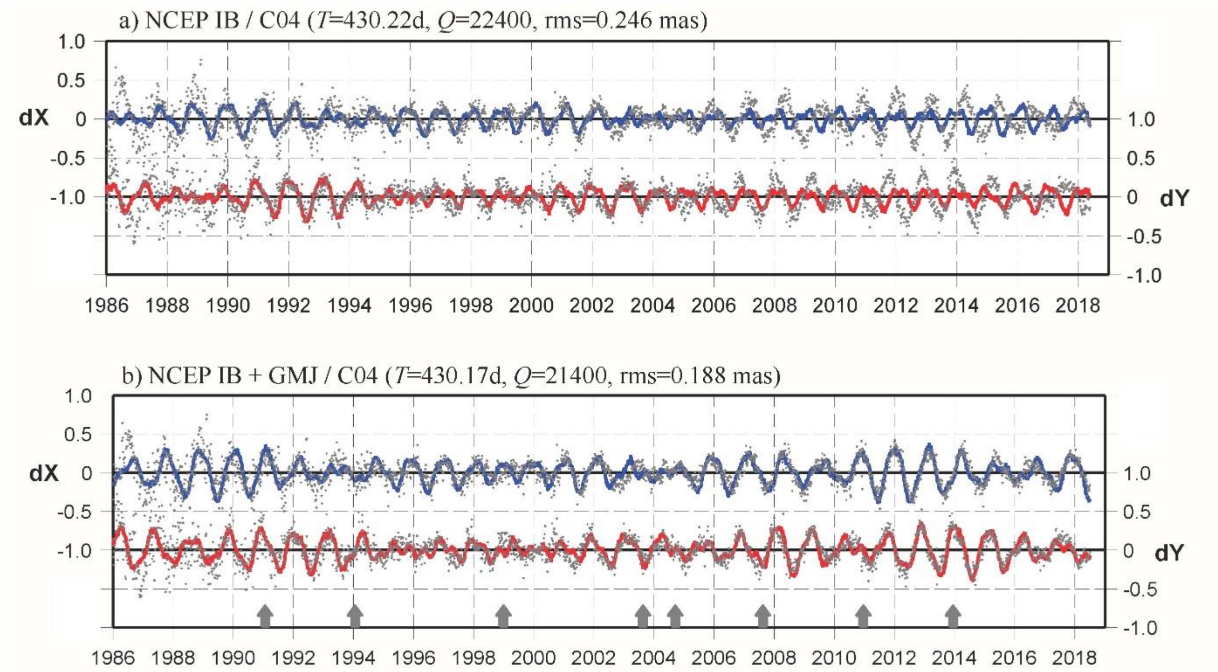

Fig. 5 Integrated (full lines) and observed (dots) CPO. Atmospheric excitations with inverted barometers correction IERS IB are used.

Finally, we compare our results with those obtained by some other authors in Table 2. Remark in the last column concerns the method used in the analysis. Only the best solutions of this paper (made with IERS C04 CPO and GMJ effects) are displayed in the last row. All periods are expressed in mean solar days.

The results presented in Table 2 do not differ very much, periods are mostly consistent within several tenths of a day and Q-factor within ten per cent of its value. Significantly different are only the results by Rosat and Lambert (2009) from gravity observations.

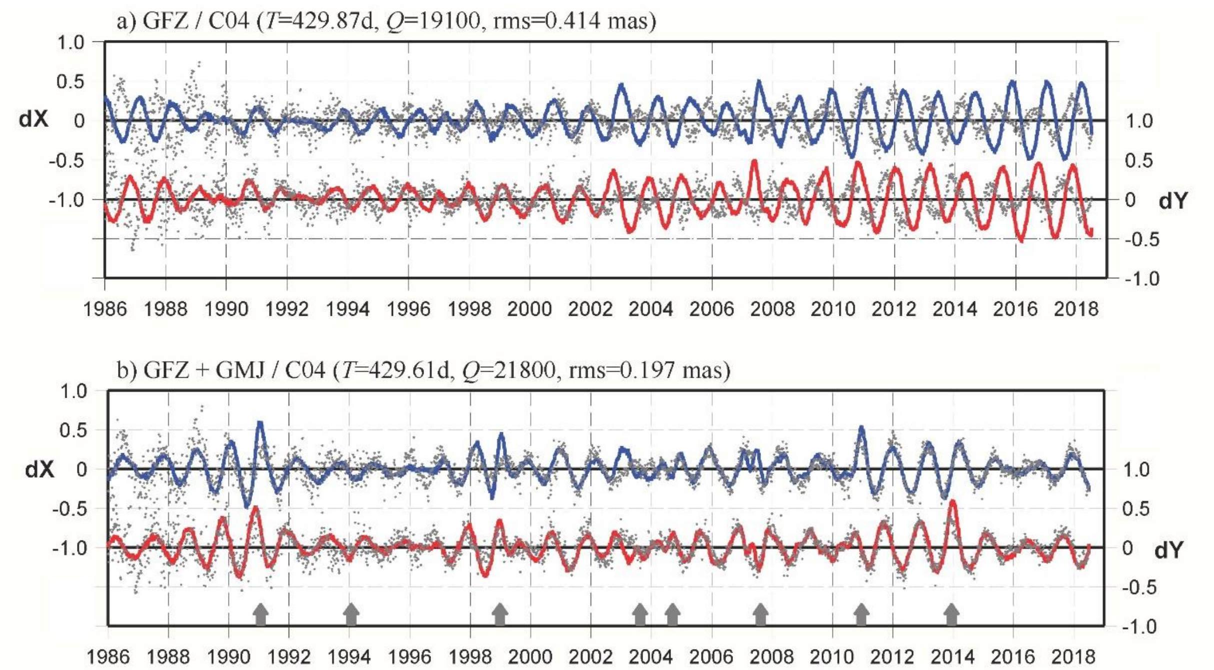

Fig. 6 Integrated (full lines) and observed (dots) CPO. Atmospheric and oceanic excitations from GFZ are used.

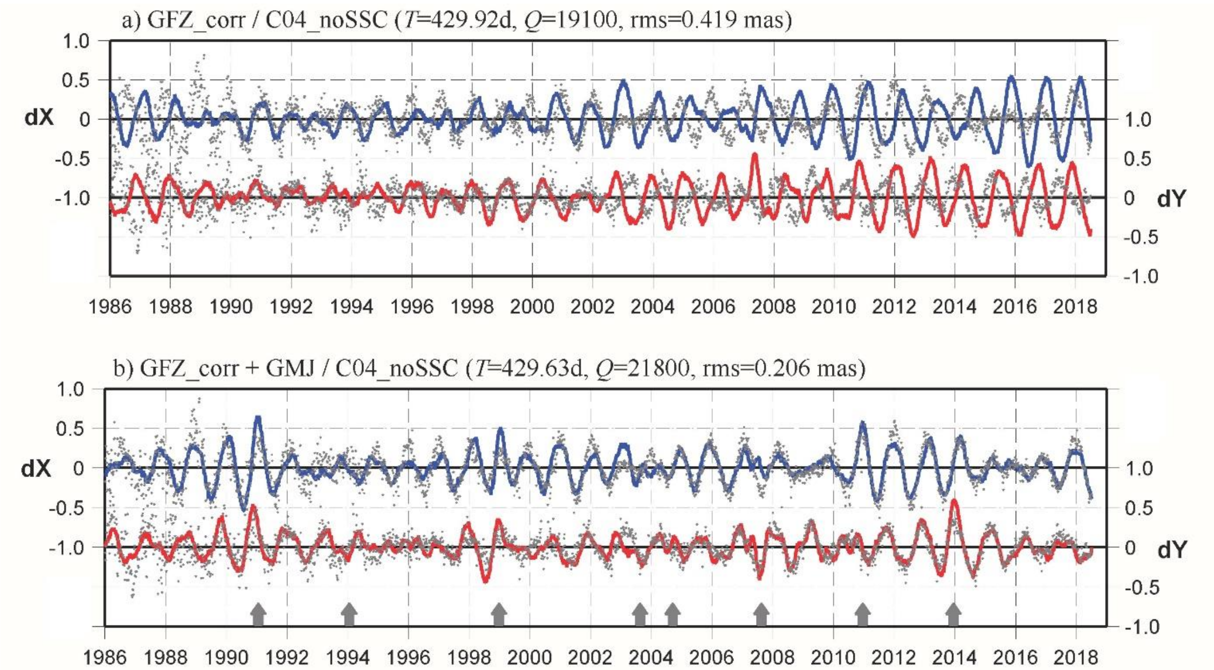

Fig. 7 Integrated (full lines) and observed (dots) CPO. Atmospheric and oceanic excitations from corrected GFZ and C04 CPO with SSC removed are used.

5. CONCLUSIONS

All results based on different VLBI solutions agree at the level of their formal uncertainties, if the same excitation model is used. The best rms fit to observations is always obtained with IERS C04 solution of CPO, but different models of excitation yield values of FCN parameters whose differences often exceed their formal errors. Existing models of atmospheric and oceanic excitations are still not sufficiently consistent, they differ significantly. Quite surprisingly, the best fit is achieved when atmospheric and oceanic excitations are neglected, and only GMJ

Table 2 Comparison of determination of FCN parameters by selected authors.

Solution	Period *T* [days]	*Q*-factor	Remark
Defraigne et al., 1994	432.9	54000	2
Florsh and Hinderer, 2000	428	10^5	2
Mathews et al., 2002	430.21	20000	3
Vondrák et al., 2005	430.55	19900	3
Rosat and Lambert, 2009	429.6	16683	3
	426.9	16630	2
Koot and de Viron, 2011	429.09	19641	3
	429.55	19416	4, with mean atmosphere
	429.82	19042	4, with variable atmosphere
Huang et al., 2011	432.34	n/a	3, without elmg. Coupling
	431.96		3, with elmg. Coupling
Krásná et al., 2013	430.00	n/a	3
Zhou et al., 2016	428.8 – 434.3	n/a	1, sliding window
Vondrák and Ron, 2017	430.28	19500	4, GMJ only
	430.16	21400	4, NCEP IB + GMJ
	429.96	19800	4, ERA/OMCT + GMJ
This paper	430.23	19600	4, GMJ only
	430.17	21400	4, NCEP IB + GMJ
	429.61	21800	4, GFZ + GMJ
	429.63	21800	4, GFZ_corr + GMJ, no SSC

Remarks:
1 spectral analysis of VLBI-based CPO (direct approach)
2 gravimetrically observed and theoretical tides
3 VLBI-observed and theoretical rigid-Earth nutation terms (indirect resonance approach)
4 same as 3 plus geophysical excitations

effects are considered. The estimated amplitudes of GMJ excitations are comparable to the excitations by atmosphere and oceans – they reach about a half of the maximum peaks of atmospheric/oceanic excitations. Inclusion of GMJ effect always improves the fit significantly, so excitations by GMJ are probably more important for exciting FCN than the ones caused by atmosphere and oceans. The largest improvement occurs in case of ESM GFZ excitations. In case when diurnal tidal atmospheric components are restored in ESM GFZ excitations, the fit to observed CPO is only slightly worse (see the last two rows of Tab.1); better fit is obtained if SSC is removed from CPO.

The estimated amplitudes of GMJ are larger when atmospheric/oceanic excitations are stronger. So it seems that required GMJ excitations partly compensate the influence of atmosphere and oceans to yield the best fit with observed CPO. In some cases, the inclusion of GMJ effect brings about relatively large changes of FCN parameters, exceeding their formal errors. However, this effect is still highly hypothetic since the exact mechanism remains unclear. A possible explanation is that GMJ gives rise to the change of electromagnetic coupling at CMB, which in turn contributes to the variation in the frequency and amplitude of FCN. The conclusions about their exact relationship cannot be made so far, as discussed recently by Cui et al. (2018, 2020).

ACKNOWLEDGEMENTS

This study was carried out thanks to the project RVO:67985815. The authors express their sincerest thanks to both reviewers, Henryk Dobslaw and an anonymous one, for their valuable comments concerning the use of ESM GFZ excitations and our analysis method.

REFERENCES

Brown, W, Beggan C, and Macmillan, S.: 2016, Geomagnetic jerks in the Swarm Era. SP-740 Proceedings of Living Planet Symposium, 9–13 May 2016. Spacebooks Online

Brzeziński, A.: 1994, Polar motion excitation by variations of the effective angular momentum function: II. Extended model. Manuscr. Geodaet., 19, 157–171.

Chao, B.F. and Hsieh, Y.: 2015, The Earth's free core nutation: Formulation of dynamics and estimation of eigenperiod from the very-long-baseline interferometry data. Earth Planet. Sci. Lett., 432, 483-492. DOI: 10.1016/j.epsl.2015.10.010

Chulliat, A. and Maus, S.: 2014, Geomagnetic secular acceleration, jerks, and a localized standing wave at the core surface from 2000 to 2010. J. Geophys. Res. Solid Earth, 119, 1531–1543. DOI: 10.1002/2013JB010604

Cui, X., Sun, H., Xu, J., Zhou, J. and Chen, X.: 2018, Detection of free core nutation resonance variation in Earth tide from global superconducting gravimeter observations. Earth Planets Space, 70, 199. DOI: 10.1186/s40623-018-0971-9

Cui, X., Sun, H., Xu, J., Zhu, J. and Chen, X.: 2020, Relationship between free core nutation and geomagnetic jerks. J. Geod., 94, 38. DOI: 10.1007/s00190-020-01367-7

Defraigne, P., Dehant, V. and Hinderer, J.: 1994, Stacking gravity tide measurements and nutation observations in order to determine the complex eigenfrequency of the nearly diurnal free wobble. J. Geophys. Res., 99, 9203–9213. DOI: 10.1029/94JB00133

Dobslaw, H. and Dill, R.: 2018, Predicting earth orientation changes from global forecasts of atmosphere-hydrosphere dynamics. Adv. Space Res., 61, 4, 1047–1054. DOI: 10.1016/j.asr.2017.11.044

Dobslaw, H. and Dill, R.: 2019, Product description document effective angular momentum functions from Earth System Modelling at GeoForschungsZentrum in Potsdam, http://rz-vm115.gfz-potsdam.de:8080/repository

Florsch, N. and Hinderer, J.: 2000, Bayesian estimation of the free core nutation parameters from the analysis of precise tidal gravity data. Phys. Earth Planet. Inter., 117, 21–35. DOI: 10.1016/S0031-9201(99)00084-9

Gross, R.S.: 2009, An improved empirical model for the effect of long-period ocean tides on polar motion. J. Geod., 83, 635–644. DOI: 10.1007/s00190-008-0277-y

Gubanov, V.S.: 2010, New estimates of retrograde free core nutation parameters. Astron. Lett., 36, 444–451. DOI: 10.1134/S1063773710060083

Hinderer, J., Boy, J.P., Gegout, P., Defraigne, P., Roosbeek, F. and Dehant, V.: 2000, Are the free core nutation parameters variable in time? Phys. Earth Planet. Inter., 117, 37–49. DOI: 10.1016/S0031-9201(99)00085-0

Huang, C.L., Dehant, V., Liao, X.H., Van Hoolst, T. and Rochester, M.G.: 2011, On the coupling between magnetic field and nutation in a numerical integration approach. J. Geophys. Res., 116, B03403. DOI:10.1029/2010JB007713

Jungclaus, J.H., Fischer, N., Haak, H., Lohmann, K., Marotzke, J., Matei, D., Mikolajewicz, U., Notz, D. and von Storch, J.S.: 2013, Characteristics of the ocean simulations in the Max Planck Institute Ocean Model (MPIOM) the ocean component of the MPI-Earth system model. J. Adv. Model. Earth Syst. 5, 422–446. DOI: 10.1002/jame.20023

Koot, L. and de Viron, O.: 2011, Atmospheric contribution to nutation and implications for the estimation of deep Earth’s properties from nutation observations. Geophys. J. Int., 185, 1255–1265. DOI: 10.1111/j.1365-246X.2011.05026.x

Krásná, H., Böhm, J. and Schuh, H.: 2013, Free core nutation observed by VLBI. Astron. Astrophys., 555, A29. DOI: 10.1051/0004-6361/201321585

Malkin, Z.: 2013, Free core nutation and geomagnetic jerks. J. Geodyn., 72, 53–58. DOI: 10.1016/j.jog.2013.06.001

Mandea, M., Holme, R., Pais, A., Pinheiro, K., Jackson, A. and Verbanac, G.: 2010, Geomagnetic jerks: Rapid core field variations and core dynamics. Space Sci. Rev., 155, 147–175. DOI: 10.1007/s11214-010-9663-x

Mathews, P.M., Herring, T.A. and Buffet B.A.: 2002, Modeling of nutation-precession for nonrigid Earth, and insights into the Earth’s interior. J. Geophys. Res., 107, B4. DOI: 10.1029/2001JB000390

Olsen, N. and Mandea, M.: 2008, Rapidly changing flows in the Earth's core. Nature Geosci., 1, 390–394. DOI: 10.1038/ngeo203

Rosat, S. and Lambert, S.B.: 2009, Free core nutation resonance parameters from VLBI and superconducting gravimeter data. Astron. Astrophys., 503, 287–291. DOI: 10.1051/0004-6361/200811489

Schindelegger, M., Böhm, S., Böhm, J. and Schuh, H.: 2013, Atmospheric effects on Earth rotation. In: Böhm. J. and Schuh, H. (Eds.): Atmospheric effects in space geodesy. Springer, 181–231. DOI: 10.1007/978-3-642-36932-2

Souchay, J., Loysel, B., Kinoshita, H. and Folgueira, M.: 1999, Corrections and new developments in rigid Earth nutation theory III. Final tables "REN-2000" including crossed-nutation and spin-orbit coupling effects. Astron. Astrophys. Suppl. Ser., 135, 111–131. DOI: 10.1051/aas:1999446

Vondrák, J.: 1977, Problem of smoothing observational data II. Bull. Astron. Inst. Czechosl., 28, 84–89.

Vondrák, J. and Ron, C.: 2015, Earth orientation and its excitations by atmosphere, oceans, and geomagnetic jerks. Serb. Astron. J., 191, 59–66. DOI: 10.2298/SAJ1591059V

Vondrák, J. and Ron, C: 2017, New method for determining free core nutation parameters, considering geophysical effects. Astron. Astrophys., 604, A56. DOI: 10.1051/0004-6361/201730635

Vondrák, J. and Ron, C: 2019, New GFZ effective angular momentum excitation functions and their impact on nutation. Acta Geodyn, Geomater., 16, 151–155. DOI: 10.13168/AGG.2019.0012

Vondrák, J., Weber, R. and Ron, C.: 2005, Free core nutation: direct observations and resonance effects. Astron. Astrophys., 444, 297–303. DOI: 10.1051/0004-6361:20053429

Zhou, Y.H., Salstein, D.A.and Chen, J.L.: 2006, Revised atmospheric excitation function series related to Earth’s variable rotation under consideration of surface topography. J. Geophys. Res., 111, D12108, DOI: 10.1029/2005JD006608

Zhou, Y.H., Zhu, Q., Salstein, D.A., Xu, X.Q., Shi, S. and Xiao, X.H.: 2016, Estimation of the free core nutation period by the sliding- complex least-squares fit method. Adv. Space Res., 57, 2136–2140. DOI: 10.1016/j.asr.2016.03.028